THE JOURNAL OF IMMUNOLOGY

The Exonuclease Trex1 Restrains Macrophage Proinflammatory Activation

Selma Pereira-Lopes, Teja Celhar, Gloria Sans-Fons, Maria Serra, Anna-Marie Fairhurst, Jorge Lloberas and Antonio Celada

J Immunol 2013; 191:6128-6135; Prepublished online 11 November 2013;
doi: 10.4049/jimmunol.1301603
http://www.jimmunol.org/content/191/12/6128

The Journal of Immunology is published twice each month by
The American Association of Immunologists, Inc.,
9650 Rockville Pike, Bethesda, MD 20814-3994.

Print ISSN: 0022-1767 Online ISSN: 1550-6606.

The Exonuclease Trex1 Restrains Macrophage Proinflammatory Activation

Selma Pereira-Lopes,* Teja Celhar,† Gloria Sans-Fons,* Maria Serra,* Anna-Marie Fairhurst,† Jorge Lloberas,* and Antonio Celada*

The three-prime repair exonuclease 1 (TREX1) is the most abundant exonuclease in mammalian cells. Mutations in *Trex1* gene are being linked to the development of Aicardi–Goutières syndrome, an inflammatory disease of the brain, and systemic lupus erythematosus. In clinical cases and in a *Trex1*-deficient murine model, chronic production of type I IFN plays a pathogenic role. In this study, we demonstrate that *Trex1*$^{-/-}$ mice present inflammatory signatures in many different organs, including the brain. Trex1 is highly induced in macrophages in response to proinflammatory stimuli, including TLR7 and TLR9 ligands. Our findings show that, in the absence of Trex1, macrophages displayed an exacerbate proinflammatory response. More specifically, following proinflammatory stimulation, *Trex1*$^{-/-}$ macrophages exhibited an increased TNF-α and IFN-α production, higher levels of CD86, and increased Ag presentation to CD4$^+$ T cells, as well as an impaired apoptotic T cell clearance. These results evidence an unrevealed function of the Trex1 as a negative regulator of macrophage inflammatory activation and demonstrate that macrophages play a major role in diseases associated with Trex1 mutations, which contributes to the understanding of inflammatory signature in these diseases. *The Journal of Immunology*, **2013, 191: 6128–6135.**

Three-prime repair exonuclease 1 (TREX1) is a homodimeric exonuclease (1–3) that degrades DNA in a 3′→5′ manner (4). TREX1 activity has a propensity toward certain DNA sequences and requires magnesium and manganese in the active site for proper functioning (5). In humans, mutations in TREX1 are associated with the Aicardi–Goutières syndrome (AGS), a neurologic disease characterized by chronic production of IFN in the CNS (6). Such mutations are also associated with familial chilblain lupus (7) and with systemic lupus erythematosus (SLE), both of which have partial symptom overlap with AGS phenotype (8). About 0.5% of SLE patients have mutations in TREX1, which indicates that mutations in this gene are the most commonly known monogenic cause for SLE (9).

The mechanism by which TREX1 deficiency leads to a disease is still not entirely clear. The mouse model, *Trex1*$^{-/-}$, has a dramatically reduced life expectancy due to the development of inflammatory myocarditis (10). An increase of intracellular DNA triggers IFN-αβ production that causes a so-called antiviral state (11), which, in turn, leads to autoimmunity. There are currently two predominant explanations for DNA origin. First, it has been shown that TREX1 deficiency impairs G_1/S cell cycle transitions. This, in turn, leads to the accumulation of ssDNA produced in S phase (12). Second, alternative evidence shows that ssDNA originates from the replication of endogenous retroelements being accumulated in Trex1-deficient mice (13). In fact, it has been found that Trex1 also neutralizes part of the function of endogenous retroelements in synovial fibroblasts, which in consequence leads to rheumatoid arthritis when Trex1 is not present (14).

The IFN-αβ production, which contributes to the above-mentioned, has been shown to be dependent on stimulator of IFN genes (STING) pathway (15). In addition, according to further studies, TBK1, IFN regulatory factor (IRF)3, and IRF7 are also required for the expression of the antiviral genes when TREX1 is absent or nonfunctional (16).

Pattern-recognition receptors when triggered lead to an innate immune activation by inducing cytokine and IFN expression (17). More precisely, in the case of nucleotides being the trigger, TLR7 recognizes ssRNA, whereas TLR9 recognizes hypomethylated CpG DNA. Both TLR7 and TLR9 trigger IRF7 and NF-κB and induce the expression of type I IFN and cytokines, respectively. In SLE and other autoimmune diseases, a plethora of immune cells are dysfunctional, including T and B cells, which together result in high levels of circulating autoreactive Abs (18). Macrophages from SLE patients are more active, with increased cytokine production and an increase in the ability to present self-Ags to T cells, together with a decreased ability to perform apoptotic clearance (19).

Our work shows that, in mice, Trex1 has a different tissue distribution with higher expression in macrophages after proinflammatory activation when comparing with other cell types as B and T cells. In the current investigation, we examined the role of Trex1 in activated macrophages. In brief, our findings show that Trex1 is required for the correct function of macrophages. Defi-

*Grupo Biología del Macrófago, Departamento de Fisiología e Inmunología, Universitat de Barcelona, 08028 Barcelona, Spain; and †Singapore Immunology Network, Immunos, Singapore 138648, Singapore

Received for publication June 17, 2013. Accepted for publication October 2, 2013.

This work was supported by Ministerio de Educación, Cultura y Deporte Formación del Profesorado Universitario Proyecto AP2010-5396 (to S.P.-L.), European Molecular Biology Organization Short Term Fellowship ASTF 206-2012 (to S.P.-L.), Ministerio de Economía y Competividad Grants BFU2007-63712/BMC and BFU2011-23662 (to A.C.), and European Union's Seventh Framework Programme (FP7/2007-2013) Grant 241779 (Nuclease Immune Mediated Brain and Lupus-Like Conditions: natural history, pathophysiology, diagnostic, and therapeutic modalities with application to other disorders of autoimmunity). This work was also supported by core funding from the Singapore Immunology Network at A*STAR, Singapore (to A.-M.F.).

Address correspondence and reprint requests to Prof. Antonio Celada, University of Barcelona, Baldiri Reixac 10, 08028 Barcelona, Spain. E-mail address: acelada@ub.edu

The online version of this article contains supplemental material.

Abbreviations used in this article: AGS, Aicardi–Goutières syndrome; BMDDC, bone marrow–derived dendritic cell; BMDM, bone marrow–derived macrophage; IRF, IFN regulatory factor; qPCR, quantitative PCR; SLE, systemic lupus erythematosus; STING, stimulator of IFN gene; TREX1, three-prime repair exonuclease 1; WT, wild type.

www.jimmunol.org/cgi/doi/10.4049/jimmunol.1301603

ciency results in a more proinflammatory phenotype characterized by increased cytokine production and increased capacity to activate T cells. Furthermore, the loss of Trex1 weakens the macrophage ability to perform an apoptotic clearance. This lack of autoregulation may explain the generalized inflammation associated with deficiency.

Materials and Methods

Mice

C57BL6J mice were purchased at Charles River Laboratories (Wilmington, MA). *Trex1*$^{-/-}$ mice (10) were provided by D. Bonthron (University of Leeds). OTII mice expressing transgenic TCRs specific for I-A^{b} plus OVA$_{323–339}$ were provided by J. L. Rodriguez (Centro de Investigaciones Biologicas, Consejo Superior de Investigaciones Cientificas, Madrid, Spain). The generation of *Tlr9*-deficient mice has been described earlier (20). Mice were at least eight generations C57BL6J; therefore, C57BL6J were used as wild type (WT). All mice were maintained and used in a specific pathogen-free facility at the Parc Cientific de Barcelona or the Biological Resource Centre in Singapore. The care and use of laboratory animals conformed to the National Institutes of Health guidelines, and all experimental procedures conformed to an Institutional Animal Care and Use Committee–approved animal protocol (Animal Research Committee of the Government of Catelonia, number 2523; A*STAR BRC IACUC 100539).

Reagents

Murine rIFN-γ, rIFN-α, rTNF-α, rIL-4, and rIL-10 were purchased from R&D Systems (Minneapolis, MN). CpGB and R848 were obtained from InvivoGen (San Diego, CA). OVA was purchased from Hyglos. All other chemicals used were of the highest available purity grade and were purchased from Sigma-Aldrich (St. Louis, MO).

Histochemistry

Animals were euthanized, and tissues were fixed in 4% paraformaldehyde and paraffin embedded. H&E sections were measured, and the grade of mononuclear inflammatory infiltration was semiquantified by using an ordinal scale as follows: −, minimal or no evidence of mononuclear infiltration; +, mild mononuclear infiltration; ++, moderate to severe mononuclear infiltration; and +++, severe mononuclear infiltration.

Cell culture and purification

Mouse fibroblasts (L929 cell line from American Type Culture Collection) were maintained in DMEM 10% heat-inactivated FCS supplemented with 2-ME and flutamax from Invitrogen (Carlsbad, CA), supplemented with 100 U/ml penicillin and 100 μg/ml streptomycin. Bone marrow–derived macrophages (BMDM) were generated from 6- to 8-wk-old mice. Bone marrow cells from femora and tibia were flushed and cultured in plastic tissue culture dishes (150 mm) in DMEM containing 20% FCS (PAA Laboratories, Pasching, Austria) and 30% of L-cell conditioned media as a source of M-CSF (21). Media was supplemented with 100 U/ml penicillin and 100 μg/ml streptomycin. Cells were incubated at 37˚C in a humidified 5% CO_2 atmosphere. After 7 d of culture, a homogeneous population of adherent macrophages was obtained (>99% CD11b and F4/80). To obtain bone marrow–derived dendritic cells (BMDDC), bone marrow cells were incubated in DMEM containing 10% FCS with GM-CSF (20 ng/ml). On days 3, 6, and 8, fresh media was added to cells. On day 10, cells were recovered (22).

Peritoneal macrophages were obtained by lavage following euthanasia. Cells were cultured in 10% FCS DMEM for 3 h at 37˚C to enable adherence of macrophages. All nonattached cells were washed using warm DMEM. Purity of the macrophage population was determined by flow cytometry (>90% CD11b and F4/80).

T and B cells were sorted from fresh spleen, using CD3-allophycocyanin Cy7 and B220-AF700, respectively, from eBioscience. Sorting was performed using a BD FACSAria SORP.

RNA extraction and real-time RT-PCR

Total RNA was extracted with Tri Reagent, purified, and DNase treated with PureLink RNA Mini Kit, as described by the manufacturer (Ambion, Life Technologies). For cDNA synthesis, 400 ng total RNA and Moloney murine leukemia virus reverse-transcriptase RNase H Minus, Point Mutant, oligo $(dT)_{15}$ primer, and PCR nucleotide mix were used, as described by the manufacturer (Promega). Quantitative PCR (qPCR) was performed in triplicate using the SYBR Green Master Mix (Applied Biosystems) in a final volume of 10 μl using a 7900 HT Fast Real Time PCR System (Applied Biosystems). Data were normalized to the housekeeping gene, *hprt1* and/or *l14*. Data are expressed as relative mRNA levels compared with the untreated control. Sequences of primers used are detailed in Supplemental Table I.

Western blot protein analysis

Cells were lysed, as described (23), in lysis buffer (1% Triton X-100, 10% glycerol, 50 mM HEPES [pH 7.5], 150 mM NaCl, protease inhibitors, and 1 mM sodium ortovanadate). After 20 min of rotation at 4˚C, cell extracts were centrifuged at 12,000 × *g* and supernatants were kept at −80˚C. Protein concentration was measured by the Bio-Rad protein analysis kit. A total of 20 μg protein extracts was heated at 95˚C in Laemmli SDS loading buffer, resolved by SDS-PAGE, and transferred to polyvinylidene difluoride membranes (Amersham). Membranes were blocked with PBS with 5% of dry milk for 1 h and then incubated with Abs against Trex1 and β-actin. Secondary Abs were peroxidase-labeled anti-mouse. ECL (Amersham) was used for detection.

TNF-α and IL-6 were detected in supernatant using Mouse ELISA Ready-SET-Go (eBioscience).

Flow cytometry

On day 7, BMDM were collected and 5 × 10^5 cells were used to assess the phenotype with flow cytometry using anti–CD115-PE, anti–F4/80-PECy5, anti–CD45-PECy7, anti–CD11b-allophycocyanin, and anti–GR1-allophycocyanin Cy7 Abs from eBioscience plus DAPI to gate out dead cells. To determine changes in expression of surface markers after activation, cells were plated in 12-well plates, left to adhere, and treated with different stimuli for 21 h. Anti–CD86-PECy7 and anti–CD40-allophycocyanin were used to detect activation levels after stimulation. Samples were acquired in BD LSRFortessa, BD FACSCanto II, or Gallios flow cytometer from Beckman Coulter depending on experimental design and availability.

Phagocytosis

Jurkat cells were washed three times in plain RPMI 1640 media and stained with CFSE (Molecular Probes, Life Technologies) at 1.25 μM for 10 min. For inducing apoptosis, labeled cells were incubated with 30 μM etoposide for 18 h. Apoptosis level was assessed with the Annexin V Apoptosis Detection Kit APC (eBioscience) (Supplemental Fig. 1). Apoptotic cells were incubated with stimulated macrophages at a ratio 4:1 (apoptotic cells: macrophage) after 1 h, media was discarded, and macrophages were collected by scraping on ice. Macrophages were stained on ice with specific Abs anti–CD45-PECY7, anti–CD11b-allophycocyanin Cy7, or anti–Ly108-PE plus DAPI to distinguish live and dead cells. Macrophages and T cells were acquired and analyzed using FlowJo. The percentage of CD11b- and CFSE-positive macrophages was used as a measure of phagocytosis.

T cell proliferation

Macrophages were plated in 96-well plate at a concentration of 5 × 10^4 cells/well. Macrophages were left to attach for 4 h and stimulated for 18 h with LPS, CpGB, or R848. Media was removed, and cells were washed once and then pulsed with 100 μg/ml OVA for 3 h; then 5 × 10^5 of CFSE-stained splenocytes from OTII mice were added to each well. After 5-d incubation period, the proliferation of T cells was assessed by flow cytometry. Cells were stained with anti–CD4-PerCpCy5.5, anti–Vα2-allophycocyanin, and anti–CD45-PECy7, as well as with DAPI for discrimination between live and dead cells.

Statistical analysis

Data were analyzed by using a two-tailed Student *t* test for comparing two groups or ANOVA for multiple groups. Bonferroni post hoc correction was used to compare pairs. Statistical analysis was performed with GraphPad Software Prism 4.

Results

Trex1$^{-/-}$ *mice have systemic inflammation*

Trex1$^{-/-}$ mice were originally reported to have a mortality rate of 50% at 20 wk of age, due to myocarditis (10). More recently, the $t_{1/2}$ has been reported to be just 10 wk, with multiple organs exhibiting extensive inflammation (15). This may suggest that

housing conditions may alter the pathological impact of *Trex1* deficiency.

Given the difference in pathology between the studies, we undertook an anatomopathological study of *Trex1*$^{-/-}$ mice to better understand the phenotypes present when these knockout mice were kept in our specific pathogen-free animal facility. To that end, *Trex1*$^{-/-}$ and WT littermates (controls) were euthanized at 6–8 wk old, and the extent of mononuclear infiltration was measured in different tissues using H&E staining (Fig. 1A, Table I). Examination of the heart demonstrated severe diffuse lymphocytic infiltration (Fig. 1A). This was more prominent in the myocardium of the left ventricle and atrium and less so in the right ventricle (data not shown). We also observed a moderate to severe mononuclear inflammatory infiltration in multiple organs, including the lung, the liver, the smooth muscle of the uterus, and the salivary gland with periductal infiltration. Inflammatory infiltration was minimal to mild in other tissues and organs, including skeletal muscle, lamina propia of glandular stomach, and lamina propia of urinary bladder, kidney, pancreas, and brain of *Trex1*$^{-/-}$ mice.

Given the fact that humans with AGS present severe encephalopathy, we decided to examine the brain further, hypothesizing that the effects of Trex1 deletion may be evident prior to pathological presentation. We determined that brain tissue from *Trex1*$^{-/-}$ mice had increased expression of *Il1β*, *Tnfα*, *Nos2*, and *cxcl10* compared with controls (Fig. 1B).

Trex1 is highly expressed in macrophages after proinflammatory activation

Due to the varying levels of cellular infiltration and inflammation in different organs, we decided to define in detail the anatomical distribution of *Trex1*. RNA expression of different C57BL6J mouse tissues was determined by qPCR. Our results show that *Trex1* is expressed in all tissues tested to some degree, and that the spleen, thymus, and uterus express the higher levels when compared with the remaining tissues examined (Fig. 2A).

Given the differing levels of Trex1 within tissues, we decided to examine the expression in purified cell populations using qPCR.

Table I. Histological mononuclear infiltration observed in the different tissues and organs of Trex1$^{-/-}$ animals

Tissue/Organ	Animal 1	Animal 2	Animal 3	Mean
Psoas muscle	+	+	+	+
Masseter muscle	+	+	+	+
Brachial muscle	+	−	−	− to +
Salivary gland	++	−	+	+ to ++
Lung	++	++	+	++
Brown adipose tissue	+++	++	++	++ to +++
Heart	+++	+++	++	+++
Pancreas	++	−	+	+
Gut	−	−	−	−
Glandular stomach	+	+	+	+
Nonglandular stomach	−	−	−	−
Liver	++	+	+	+ to ++
Gall bladder	−	−	−	−
Kidney	+	−	+	+
Urinary bladder	+	−	+	+
Uterus	++	ND	ND	++
Coagulative gland	ND	+	+	+
Brain	−	−	−	−

Four intensity levels have been defined, as follows: −, absence of mononuclear infiltration; +, mild mononuclear infiltration; ++, moderate to severe mononuclear infiltration; and +++, severe mononuclear infiltration.

Furthermore, because *Trex1* deletion is associated with systemic inflammation, we determined expression following stimulation. *Trex1* was absent in a murine fibroblast cell line, L929, but was detected in splenic B and T cells, peritoneal macrophages, BMDDCs, and BMDMs (Fig. 2B). As a contrast, *Trex1* levels were significantly higher in all immune cells. This suggests the importance of Trex1 expression in the immune cells analyzed.

We have shown previously that *Trex1* is upregulated in macrophages following stimulation with IFN-γ (24). We therefore sought to determine whether other inflammatory stimuli could modulate Trex1 expression across multiple cell types. Interestingly, expression in T cells and fibroblasts was unaffected by all stimuli used (Fig. 2B). However, incubation with type I IFN (IFN-α) resulted in a significant upregulation of Trex1 mRNA in purified B cells, peritoneal macrophages, BMDMs, and BMDDCs

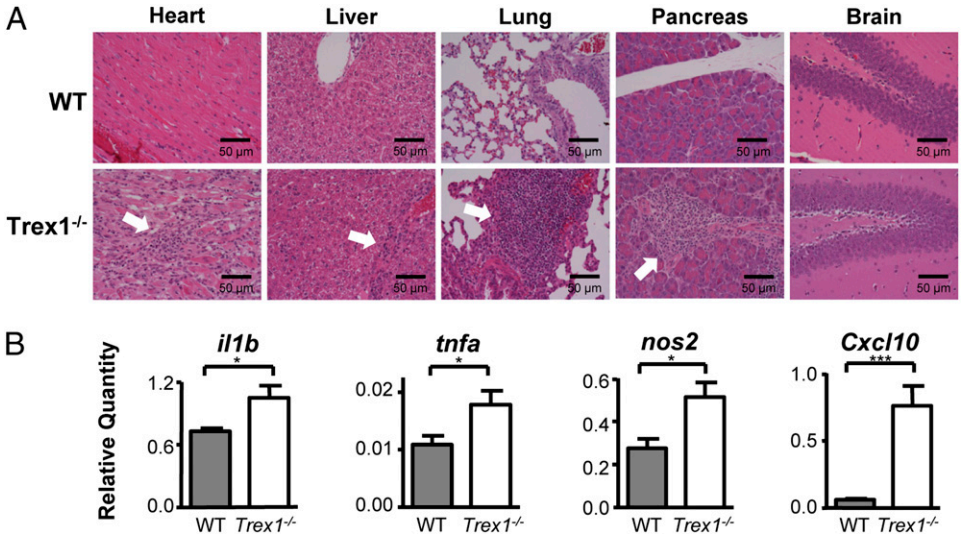

FIGURE 1. *Trex1*$^{-/-}$ mice develop multiple organ inflammation. (**A**) Representative H&E tissue sections are shown for both WT and *Trex1*$^{-/-}$ mice. Mononuclear infiltration (indicated with the white arrows) can be observed in heart, liver, lung, and pancreas sections from *Trex*$^{-/-}$ mice compared with WT, but not brain. Scale bars, 50 μm. (**B**) RNA was extracted from brains of *Trex1*$^{-/-}$ mice and controls. The level of RNA expression of the indicated genes was determined using qPCR. *Trex1*$^{-/-}$ mice brains present higher expression of proinflammatory genes in comparison with controls. All assays are representative of at least three independent experiments showing similar results. The results shown are mean ± SD. *$p < 0.05$, ***$p < 0.001$ in relation to the controls when all the independent experiments have been compared.

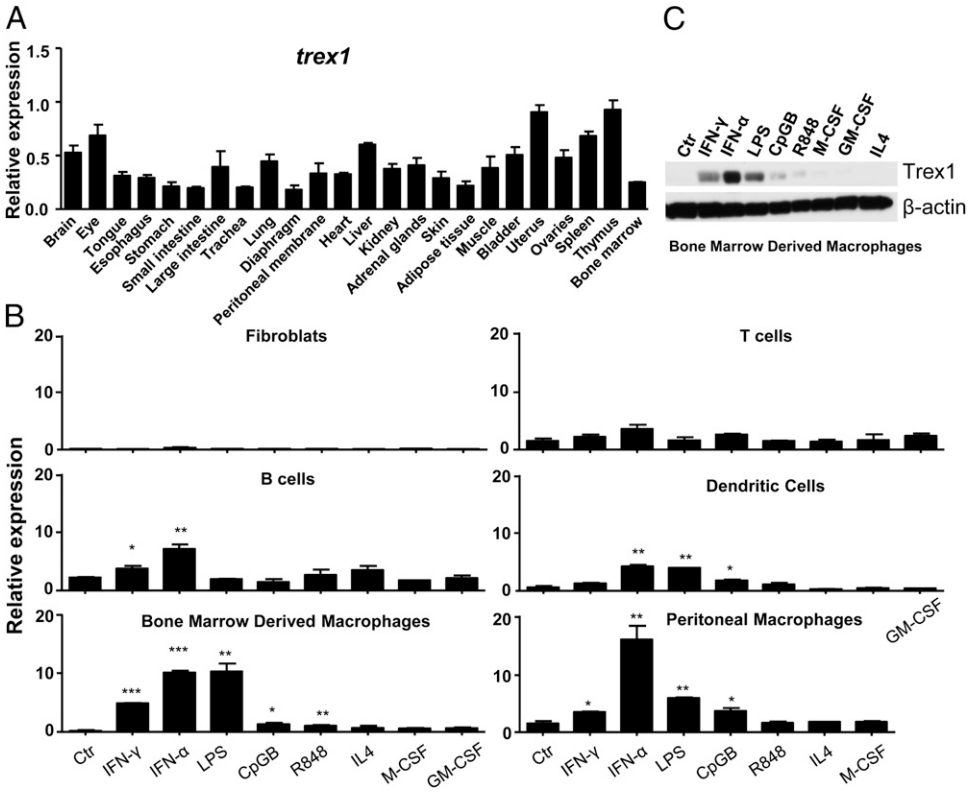

FIGURE 2. Trex1 is widely expressed in immune cells and upregulated after inflammatory stimulation in macrophages. (**A**) *Trex1* shows tissue-specific distribution. Tissues from three different C57BL6J mice were used to obtain RNA, and Trex1 expression was determined by qPCR. (**B**) *Trex1* mRNA expression in different cells under distinct conditions. Total RNA was isolated from different cells stimulated with the stimulus indicated during 6 h. (**C**) Trex1 protein in BMDM. Total protein extracts were prepared from BMDM stimulated for 24 h with the stimulus indicated and tested by Western blotting for Trex1 and β-actin expression. All assays are representative of at least three independent experiments showing similar results. $*p < 0.05$, $**p < 0.01$, $***p < 0.001$ in relation to the controls when all the independent experiments have been compared.

(Fig. 2B). Stimulation with type II IFN (IFN-γ) resulted in an increase in Trex1 expression in macrophages and B cells, but not in DCs. Dysregulation of several TLRs has been associated with the development of autoimmunity, particularly SLE. Stimulation of macrophages or DCs, but not B cells, with ligands to TLR4 (LPS), TLR7 (R848), or TLR9 (CpG-B) resulted in increased levels of Trex1, demonstrating that multiple proinflammatory stimuli can regulate Trex1 expression. However, incubation with anti-inflammatory stimuli such as IL-4, or growth factors, M-CSF, or GM-CSF had no effect on all cell types tested. Because mRNA expression may not reflect actual protein changes, we analyzed expression in BMDM using Western blot (Fig. 2C). To confirm that we did not have endotoxin contamination, we used polymyxin B while stimulating BMDM with IFN-γ, IFN-α, and LPS (as positive control) (Supplemental Fig. 2). Our data confirmed an upregulation in Trex1 protein following IFN-γ, IFN-α, and TLR stimulation.

Stimulation of TLR9 induces Trex1 in macrophages

TLR9 is one of the four intracellular pathogen-associated molecular pattern receptors that recognize pathogenic nucleic acids, specifically CpG islands present in bacteria and virus, but not in mammalian DNA. This TLR activates the immune system signaling through MyD88 activating NF-κB and IRF transcription factors (3). TLR9 deficiency has also been shown to drive SLE pathogenesis in murine models (25, 26). Furthermore, the data described above demonstrate that TLR9 signaling modulates Trex1 expression, suggesting the possibility that they exist in a regulatory feedback loop. Therefore, we went on to verify whether there was dysregulated Trex1 expression in the TLR9-deficient mice. As expected, upregulation of Trex1 by CpGB was abolished in $TLR9^{-/-}$ macrophages (Fig. 3). However, the increase in Trex1 expression following IFN-γ and LPS was unaltered in TLR9-deficient macrophages (Fig. 3A). Interestingly, we did detect an inhibition of the increase in IFN-β and TNF-α following LPS and CpG stimulation, respectively (Fig. 3B, 3C).

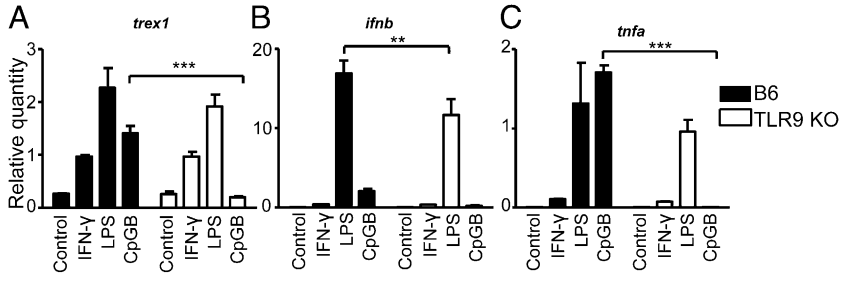

FIGURE 3. Trex1 is upregulated by TLR9 direct stimulation. Macrophages from $TLR9^{-/-}$ and control mice were treated for 6 h with different proinflammatory stimuli, and *trex1* (**A**), *ifnβ* (**B**), and *tnfα* (**C**) expression was determined. All assays are representative of at least three independent experiments showing similar results. Each point was performed in triplicate, and the results are shown as mean ± SD. $**p < 0.01$, $***p < 0.001$ in relation to the controls when all the independent experiments have been compared.

Trex1$^{-/-}$ *macrophages exhibit an exacerbated proinflammatory response*

In view of the significantly higher induction of Trex1 in macrophages compared with other immune cell types, we decided to examine whether the lack of Trex1 in this population could affect phenotype and function. We analyzed the surface expression of maturation markers in *Trex1*$^{-/-}$ and control BMDMs, which are a homogeneous population of primary quiescent cells. There were no significant differences in the surface expression of CD11b, F4/80, CD115 (also known as M-CSFR), and GR-1 (also Ly6G) if Trex1 was present or not (Fig. 4A).

We then examined the functional cytokine response of Trex1-deficient BMDMs to TLR4, TLR7, and TLR9 stimulation. LPS stimulation revealed an increase in IL-1β mRNA with a concomitant decrease in IFN-β (Fig. 4B). There were no measurable differences in the release of TNF-α or IL-6 following LPS stimulation (Fig. 4C). Further examination revealed that the increased production of TNF-α following TLR9 stimulation was augmented in BMDMs lacking Trex1 (Fig. 4C). Incubation with the TLR7 ligand (R848) resulted in increased IFN-β expression in *Trex1*$^{-/-}$ BMDMs compared with controls (Fig. 4B). The other cytokines tested did not show any significant differences. Analysis of cell surface costimulation molecules revealed a higher upregulation of CD86 following LPS stimulation in *Trex1*$^{-/-}$ BMDMs compared with controls. There were no detectable differences following TLR7 or TLR9 incubation (Fig. 4D). The presence of Trex1 did not modify the levels of CD40 following any TLR stimulation (Fig. 4D). These results suggest that Trex1 has an important role in macrophage response to proinflammatory activation.

Trex1 represses Ag presentation by activated macrophages

As absence of Trex1 in macrophages induced higher expression of CD86 (a costimulator protein in APCs), we decided to determine the ability of Trex1-deficient macrophages to induce T cell proliferation following Ag processing and presentation. To that end, we pulsed previously stimulated macrophages with OVA for 3 h. Thereafter, we added splenocytes from OTII mice (mice with a transgenic TCR that specifically recognizes the OVA 323–339 peptide) that were previously stained with CFSE. T cell proliferation was assessed by flow cytometry on day 5. We determined that, whereas there were no differences in naive macrophage Ag presentation between control and Trex1-deficient mice, macrophages from *Trex1*$^{-/-}$ mice induce significantly more T cell proliferation after stimulation with LPS and R848 (Fig. 5). These findings demonstrate the importance of Trex1 in macrophage Ag presentation that is exacerbated after specific TLR stimulation.

Trex1 is necessary for efficient phagocytosis by activated macrophages

A defect in macrophage clearance of apoptotic cells has been described in SLE patients and murine models (27). Therefore, we decided to analyze whether and to what extent the lack of Trex1 would affect this function. Macrophages from *Trex1*$^{-/-}$ and control mice were stimulated with different proinflammatory stimuli and thereafter further incubated with apoptotic CFSE-labeled T cells for 1 h, as described in *Materials and Methods*. Our results show that macrophages lacking Trex1 have an impaired phagocytic ability following overnight incubation with TLR4, TLR7, and TLR9 ligands (Fig. 6). These treatments did not affect significantly the expression of macrophage markers CD11b and Ly108. To determine whether the change in apoptotic clearance could impact the levels of released nucleic acids, we measured the DNA present in the supernatant following incubation with apoptotic cells (Supplemental Fig. 3). No significant difference was found. These data, together with our results described above, suggest that Trex1 controls the response of macrophages to TLR stimulation and has an important role in the resolution of inflammation.

Discussion

Deficiency of Trex1 in human patients and murine models is characterized by systemic inflammation, which includes autoim-

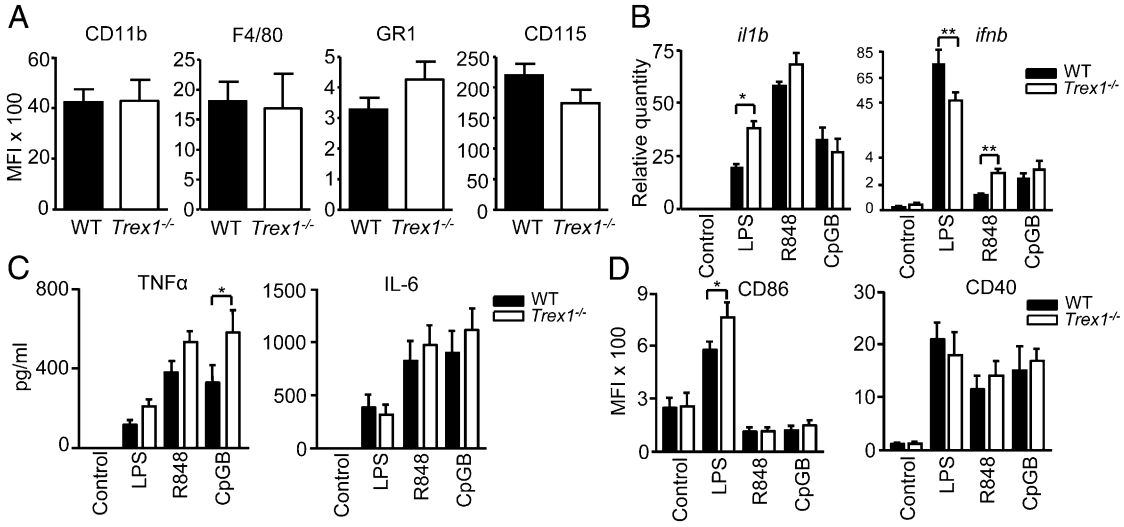

FIGURE 4. Macrophages from *Trex1*$^{-/-}$ mice produce higher levels of inflammatory cytokines in response to TLR ligands. (**A**) Macrophages obtained from *Trex1*$^{-/-}$ and control mice present similar phenotype. CD11b, F4/80, CD115, and GR1 expression were measured by flow cytometry. (**B**) Macrophages from *Trex1*$^{-/-}$ mice upregulate *il1β* to a greater extent, but regulate *ifnβ* to a lesser extent following TLR4 simulation. Incubation with R848 (TLR7 ligation) resulted in an increase of *ifnβ* by *Trex1*$^{-/-}$ macrophages. Levels of expression were determined by qPCR at 9 and 3 h for *il1β* and *ifnβ*, respectively. (**C**) Macrophages from *Trex1*$^{-/-}$ produce more TNF-α after 24-h stimulation. Supernatants were collected, and the levels of TNF-α and IL-6 were measured. (**D**) Increased expression of CD86 in macrophages of *Trex1*$^{-/-}$ mice after LPS treatment. The expression of CD86 and CD40 was determined with flow cytometry after 24-h stimulation. All assays are representative of at least three independent experiments showing similar results. Results are shown as mean ± SD. *$p < 0.05$, **$p < 0.01$ in relation to the controls when all the independent experiments have been compared.

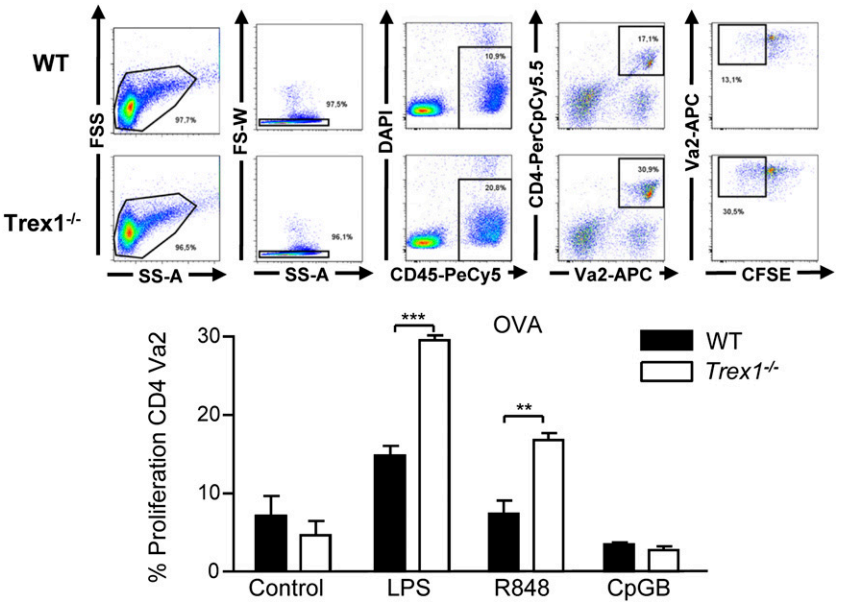

FIGURE 5. Activated macrophages from *Trex1*$^{-/-}$ mice induce increased T cell proliferation. Macrophages were stimulated for 24 h, incubated with OVA for 3 h, and then cocultured with splenocytes from OT-II mice for 5 d. Floating cells were collected, stained, and analyzed by FACS. In the *top panels*, an example is shown of the gating strategy. First and second panel gates for single cells are followed by a third panel gate where only CD45 live cells are selected. From these, the positive CD4 cells with TCR Vα2 chain were gated, and the percentage of T cell proliferating cells was determined by the loss of CFSE fluorescence, as this staining is diluted after cell proliferation. In the *bottom panels*, the mean ± SD of three independent experiments is shown. $^{**}p < 0.01$, $^{***}p < 0.001$ in relation to the controls.

munity (11). In the studies presented in this work, we demonstrate that Trex1 plays an important regulatory role in activated macrophages. Deficiency results in an increased activated proinflammatory phenotype associated with an enhanced Ag presentation. Furthermore, *Trex1*$^{-/-}$ mature macrophages exhibit a defect in the phagocytosis of apoptotic cells, which is an important mechanism for the resolution of inflammation.

Our findings also confirm and extend previous observations that *Trex1*$^{-/-}$ mice present severe inflammation at multiple sites (15), including the brain, despite measureable monocyte infiltration in this organ. In fact, recently, it has been demonstrated that in vitro IFN-α treatment promotes astrocyte activation, supporting the idea of inflammation as a key feature in the pathogenesis of AGS (28). We also showed that Trex1 has a tissue-specific distribution with the highest levels in spleen, thymus, and uterus. This may explain why the level of tissue inflammation in the mice varies across various tissues and why cardiac disease is the most frequently described trait of Trex1-deficient mice.

Examination of cellular expression revealed high levels of Trex1 in immune cells, which were highly induced by proinflammatory stimuli and not by anti-inflammatory cytokines or growth factors in macrophages. This is concurrent with the observation made in human monocyte-derived macrophages in which Trex1 was also upregulated after proinflammatory stimuli (29). Additionally, it has also been reported that Trex1 is upregulated by genotoxic drugs (30, 31), indicating that Trex1 is needed for both pathogen DNA degradation and also small strands of nuclear DNA originated from genotoxicity. This suggests that, under the normal physio-

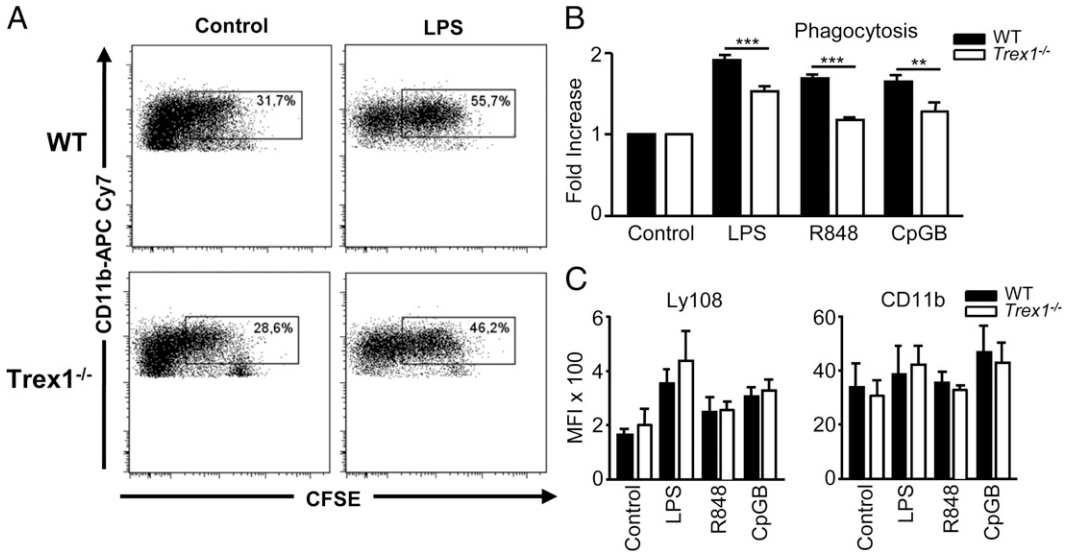

FIGURE 6. Apoptotic clearance is impaired in macrophages from *Trex1*$^{-/-}$ mice. (**A**) Apoptotic cells were labeled with CFSE (cytoplasmatic dye) and incubated with stimulated or control BMDM at a ratio of 4:1 for 1 h. Supernatant was removed and macrophages were collected, stained, and analyzed by flow cytometry. Macrophages that phagocyted apoptotic cells were detected as CFSE positive, when compared with the control (macrophages incubated with no CFSE-labeled cells). Phagocytosis values are presented as fold change of percentage of positive CFSE live macrophages. (**B**) The cumulative graphs of phagocytosis show a reduction in *Trex1*$^{-/-}$ macrophages following TLR stimulation. (**C**) The expression levels of macrophage surface markers are shown; no significant differences were seen here. All assays are representative of at least three independent experiments showing similar results. Results are shown as mean ± SD. $^{**}p < 0.01$, $^{***}p < 0.001$ in relation to the controls when all the independent experiments have been compared.

logical environment, Trex1 is upregulated following immune or genotoxicity challenge to degrade an excess of cytoplasmatic DNA and also to regulate the host immune response. This hypothesis is based upon findings demonstrating that deficiency of Trex1 increases the production of proinflammatory cytokines such as TNF-α, IFN type 1, and IL-1β following TLR ligand exposure. These *Trex1*$^{-/-}$ TLR-activated macrophages have higher levels of surface CD86 and an increased capability in Ag presentation, which leads to activation of adaptive immune system with priming autoreactive T cells. The accumulation of DNA further triggers intracellular DNA receptors as STING (32) and in consequence overactivates macrophages. Furthermore, *Trex1*$^{-/-}$ macrophages present a reduced ability to phagocyte apoptotic material. All these facts may explain the exacerbated inflammatory phenotype in Trex1-associated diseases.

Excessive macrophage activation has numerous damaging effects, exemplified in septic shock, which can lead to multiple organ dysfunction syndrome and death through a surplus of TNF-α production among other cytokines (33). In other situations, persistence of proinflammatory activity results in the development of chronic inflammation and autoimmunity. This defect is arguably related to the excessive production of type I of IFN, signature of the AGS (6) that is also associated with autoimmune diseases.

A strong activation of macrophages could result in self-damage. LPS activation of macrophages can induce apoptosis through the autocrine production of TNF-α (34). To prevent undesirable effects, macrophages have several mechanisms to protect against excessive activation that prevents their self-destruction (35). For example, CDK inhibitor p21^{Waf1} is induced by IFN-γ and protects from apoptosis (23). In the absence of this CDK inhibitor, mice develop a lupus-like phenotype characterized by anti-DNA Abs and glomerulonephritis (36, 37). p21^{Waf1} is a negative regulator that curbs excessive macrophage activation by providing a negative feedback system of TNF-α and IL-1β production (38, 39). We propose a similar function for Trex1 as macrophage controller of activation.

Impaired macrophage function, specifically with regard to the clearance of dead cells, has been widely described in both patients and murine models of SLE (40). This is an important mechanism for the resolution of inflammation. Also, this process generates circulating DNA, which is often found increased in patients with SLE (41, 42). In our system, we did not observe any differences in the release of DNA by macrophages, despite the remarkable reduction in phagocytosis by *Trex1*$^{-/-}$ macrophages, indicating that these are two independent mechanisms. Trex1 is a highly processive exonuclease potentially affecting the digestion of apoptotic DNA engulfed by macrophages. Therefore, it is possible that the uptake of external apoptotic bodies may also accumulate outside the cell, affecting the net results. Furthermore, a recent publication has described dysregulation of lysosomes associated with Trex1 deficiency that may affect apoptotic cell processing (16). This would top with further activation of the macrophage, as it is known that macrophages switch to an anti-inflammatory profile after phagocytosis of apoptotic cells (43), and the lower phagocytic capacity could contribute to a delayed switch.

A percentage of SLE patients exhibits a loss in Trex1 function (8). In addition, we have shown that both TLR7 and TLR9 (19), which have been associated with the development of SLE, upregulate Trex1, and that, in its absence, responses to these TLR ligands result in an augmented inflammatory response.

Our data demonstrate that Trex1 plays a key role in the inflammatory processes by macrophages. These cells are scavengers for apoptotic cells and, in the absence of Trex1, unprocessed DNA could induce in a STING-dependent or independent fashion the production of cytokines and the exacerbation of the immune system explaining the inflammatory process. Our data suggest that this pathway may play a role in the development of autoimmune diseases.

Acknowledgments

We wholeheartedly thank Gemma Lopez, Natalia Plana, and the staff of the Laboratory Animal Applied Research Platform of the Barcelona Science Park for excellent technical assistance. We remain indebted to all Nuclease Immune Mediated Brain and Lupus-Like Conditions Consortium members for insightful and useful comments. The Nuclease Immune Mediated Brain and Lupus-Like Conditions Consortium is composed of David Bonthron, Genetics Section, Leeds Institute of Molecular Medicine, St. James's University Hospital (Leeds, U.K.); Yanick Crow, Genetic Medicine, Manchester Academic Health Science Centre (Manchester, U.K.); Taco Kuijpers, Academic Medical Center, University of Amsterdam (Amsterdam, The Netherlands); Arn van den Maagdenberg, Departments of Human Genetics and Neurology, Leiden University Medical Centre (Leiden, The Netherlands); Simona Orcesi, Department of Child Neurology and Psychiatry, Instituto di Ricovero e Cura a Carattere Scientifico, Mondino Institute of Neurology Foundation (Pavia, Italy); Dan Stetson, Department of Immunology, University of Washington (Seattle, WA); and Adeline Vanderver, Children Research Institute (Washington, D.C.).

Disclosures

The authors have no financial conflicts of interest.

References

1. Mazur, D. J., and F. W. Perrino. 2001. Structure and expression of the TREX1 and TREX2 3′—>5′ exonuclease genes. *J. Biol. Chem.* 276: 14718–14727.
2. Brucet, M., J. Querol-Audí, M. Serra, X. Ramirez-Espain, K. Bertlik, L. Ruiz, J. Lloberas, M. J. Macias, I. Fita, and A. Celada. 2007. Structure of the dimeric exonuclease TREX1 in complex with DNA displays a proline-rich binding site for WW domains. *J. Biol. Chem.* 282: 14547–14557.
3. Kawai, T., and S. Akira. 2010. The role of pattern-recognition receptors in innate immunity: update on Toll-like receptors. *Nat. Immunol.* 11: 373–384.
4. Mazur, D. J., and F. W. Perrino. 1999. Identification and expression of the TREX1 and TREX2 cDNA sequences encoding mammalian 3′—>5′ exonucleases. *J. Biol. Chem.* 274: 19655–19660.
5. Brucet, M., J. Querol-Audí, K. Bertlik, J. Lloberas, I. Fita, and A. Celada. 2008. Structural and biochemical studies of TREX1 inhibition by metals: identification of a new active histidine conserved in DEDDh exonucleases. *Protein Sci.* 17: 2059–2069.
6. Crow, Y. J., B. E. Hayward, R. Parmar, P. Robins, A. Leitch, M. Ali, D. N. Black, H. van Bokhoven, H. G. Brunner, B. C. Hamel, et al. 2006. Mutations in the gene encoding the 3′-5′ DNA exonuclease TREX1 cause Aicardi-Goutières syndrome at the AGS1 locus. *Nat. Genet.* 38: 917–920.
7. Rice, G., W. G. Newman, J. Dean, T. Patrick, R. Parmar, K. Flintoff, P. Robins, S. Harvey, T. Hollis, A. O'Hara, et al. 2007. Heterozygous mutations in TREX1 cause familial chilblain lupus and dominant Aicardi-Goutieres syndrome. *Am. J. Hum. Genet.* 80: 811–815.
8. Lee-Kirsch, M. A., M. Gong, D. Chowdhury, L. Senenko, K. Engel, Y. A. Lee, U. de Silva, S. L. Bailey, T. Witte, T. J. Vyse, et al. 2007. Mutations in the gene encoding the 3′-5′ DNA exonuclease TREX1 are associated with systemic lupus erythematosus. *Nat. Genet.* 39: 1065–1067.
9. Stewart, A. E., S. Dowd, S. M. Keyse, and N. Q. McDonald. 1999. Crystal structure of the MAPK phosphatase Pyst1 catalytic domain and implications for regulated activation. *Nat. Struct. Biol.* 6: 174–181.
10. Morita, M., G. Stamp, P. Robins, A. Dulic, I. Rosewell, G. Hrivnak, G. Daly, T. Lindahl, and D. E. Barnes. 2004. Gene-targeted mice lacking the Trex1 (DNase III) 3′—>5′ DNA exonuclease develop inflammatory myocarditis. *Mol. Cell. Biol.* 24: 6719–6727.
11. Tanoue, T., T. Yamamoto, and E. Nishida. 2002. Modular structure of a docking surface on MAPK phosphatases. *J. Biol. Chem.* 277: 22942–22949.
12. Yang, Y. G., T. Lindahl, and D. E. Barnes. 2007. Trex1 exonuclease degrades ssDNA to prevent chronic checkpoint activation and autoimmune disease. *Cell* 131: 873–886.
13. Stetson, D. B., J. S. Ko, T. Heidmann, and R. Medzhitov. 2008. Trex1 prevents cell-intrinsic initiation of autoimmunity. *Cell* 134: 587–598.
14. Neidhart, M., E. Karouzakis, G. G. Schumann, R. E. Gay, and S. Gay. 2010. Trex-1 deficiency in rheumatoid arthritis synovial fibroblasts. *Arthritis Rheum.* 62: 2673–2679.
15. Owens, D. M., and S. M. Keyse. 2007. Differential regulation of MAP kinase signalling by dual-specificity protein phosphatases. *Oncogene* 26: 3203–3213.
16. Wang, Z., C. Zang, K. Cui, D. E. Schones, A. Barski, W. Peng, and K. Zhao. 2009. Genome-wide mapping of HATs and HDACs reveals distinct functions in active and inactive genes. *Cell* 138: 1019–1031.

17. Cao, W., C. Bao, E. Padalko, and C. J. Lowenstein. 2008. Acetylation of mitogen-activated protein kinase phosphatase-1 inhibits Toll-like receptor signaling. *J. Exp. Med.* 205: 1491–1503.
18. Celhar, T., R. Magalhães, and A. M. Fairhurst. 2012. TLR7 and TLR9 in SLE: when sensing self goes wrong. *Immunol. Res.* 53: 58–77.
19. Byrne, J. C., J. Ní Gabhann, E. Lazzari, R. Mahony, S. Smith, K. Stacey, C. Wynne, and C. A. Jefferies. 2012. Genetics of SLE: functional relevance for monocytes/macrophages in disease. *Clin. Dev. Immunol.* 2012: 582352.
20. Burkatovskaya, M., G. P. Tegos, E. Swietlik, T. N. Demidova, A. P Castano, and M. R. Hamblin. 2006. Use of chitosan bandage to prevent fatal infections developing from highly contaminated wounds in mice. *Biomaterials* 27: 4157–4164.
21. Celada, A., P. W. Gray, E. Rinderknecht, and R. D. Schreiber. 1984. Evidence for a gamma-interferon receptor that regulates macrophage tumoricidal activity. *J. Exp. Med.* 160: 55–74.
22. Lutz, M. B., N. Kukutsch, A. L. Ogilvie, S. Rössner, F. Koch, N. Romani, and G. Schuler. 1999. An advanced culture method for generating large quantities of highly pure dendritic cells from mouse bone marrow. *J. Immunol. Methods* 223: 77–92.
23. Xaus, J., M. Cardó, A. F. Valledor, C. Soler, J. Lloberas, and A. Celada. 1999. Interferon gamma induces the expression of p21waf-1 and arrests macrophage cell cycle, preventing induction of apoptosis. *Immunity* 11: 103–113.
24. Lu, T. C., Z. Wang, X. Feng, P. Chuang, W. Fang, Y. Chen, S. Neves, A. Maayan, H. Xiong, Y. Liu, et al. 2008. Retinoic acid utilizes CREB and USF1 in a transcriptional feed-forward loop in order to stimulate MKP1 expression in human immunodeficiency virus-infected podocytes. *Mol. Cell. Biol.* 28: 5785–5794.
25. Santiago-Raber, M. L., I. Dunand-Sauthier, T. Wu, Q. Z. Li, S. Uematsu, S. Akira, W. Reith, C. Mohan, B. L. Kotzin, and S. Izui. 2010. Critical role of TLR7 in the acceleration of systemic lupus erythematosus in TLR9-deficient mice. *J. Autoimmun.* 34: 339–348.
26. Hasselgren, P. O. 2007. Ubiquitination, phosphorylation, and acetylation: triple threat in muscle wasting. *J. Cell. Physiol.* 213: 679–689.
27. Xu, G., Y. Zhang, L. Zhang, A. I. Roberts, and Y. Shi. 2009. C/EBPbeta mediates synergistic upregulation of gene expression by interferon-gamma and tumor necrosis factor-alpha in bone marrow-derived mesenchymal stem cells. *Stem Cells* 27: 942–948.
28. Cuadrado, E., M. H. Jansen, J. Anink, L. De Filippis, A. L. Vescovi, C. Watts, E. Aronica, E. M. Hol, and T. W. Kuijpers. 2013. Chronic exposure of astrocytes to interferon-α reveals molecular changes related to Aicardi-Goutieres syndrome. *Brain* 136: 245–258.
29. Cobos Jiménez, V., T. Booiman, S. W. de Taeye, K. A. van Dort, M. A. Rits, J. Hamann, and N. A. Kootstra. 2012. Differential expression of HIV-1 interfering factors in monocyte-derived macrophages stimulated with polarizing cytokines or interferons. *Sci. Rep.* 2: 763.
30. Christmann, M., M. T. Tomicic, D. Aasland, N. Berdelle, and B. Kaina. 2010. Three prime exonuclease I (TREX1) is Fos/AP-1 regulated by genotoxic stress and protects against ultraviolet light and benzo(a)pyrene-induced DNA damage. *Nucleic Acids Res.* 38: 6418–6432.
31. Tomicic, M. T., D. Aasland, T. Nikolova, B. Kaina, and M. Christmann. 2013. Human three prime exonuclease TREX1 is induced by genotoxic stress and involved in protection of glioma and melanoma cells to anticancer drugs. *Biochim. Biophys. Acta* 1833: 1832–1843.
32. Gall, A., P. Treuting, K. B. Elkon, Y. M. Loo, M. Gale, Jr., G. N. Barber, and D. B. Stetson. 2012. Autoimmunity initiates in nonhematopoietic cells and progresses via lymphocytes in an interferon-dependent autoimmune disease. *Immunity* 36: 120–131.
33. Casals-Casas, C., E. Alvarez, M. Serra, C. de la Torre, C. Farrera, E. Sánchez-Tilló, C. Caelles, J. Lloberas, and A. Celada. 2009. CREB and AP-1 activation regulates MKP-1 induction by LPS or M-CSF and their kinetics correlate with macrophage activation versus proliferation. *Eur. J. Immunol.* 39: 1902–1913.
34. Xaus, J., M. Comalada, A. F. Valledor, J. Lloberas, F. López-Soriano, J. M. Argilés, C. Bogdan, and A. Celada. 2000. LPS induces apoptosis in macrophages mostly through the autocrine production of TNF-alpha. *Blood* 95: 3823–3831.
35. Valledor, A. F., M. Comalada, L. F. Santamaría-Babi, J. Lloberas, and A. Celada. 2010. Macrophage proinflammatory activation and deactivation: a question of balance. *Adv. Immunol.* 108: 1–20.
36. Balomenos, D., J. Martín-Caballero, M. I. García, I. Prieto, J. M. Flores, M. Serrano, and C. Martínez-A. 2000. The cell cycle inhibitor p21 controls T-cell proliferation and sex-linked lupus development. *Nat. Med.* 6: 171–176.
37. Salvador, J. M., M. C. Hollander, A. T. Nguyen, J. B. Kopp, L. Barisoni, J. K. Moore, J. D. Ashwell, and A. J. Fornace, Jr. 2002. Mice lacking the p53-effector gene Gadd45a develop a lupus-like syndrome. *Immunity* 16: 499–508.
38. Scatizzi, J. C., M. Mavers, J. Hutcheson, B. Young, B. Shi, R. M. Pope, E. M. Ruderman, D. S. Samways, J. A. Corbett, T. M. Egan, and H. Perlman. 2009. The cyclin dependent kinase domain of p21 is a suppressor of IL-1β-mediated inflammation in activated macrophages. *Eur. J. Immunol.* 39: 820-825.
39. Trakala, M., C. F. Arias, M. I. García, M. C. Moreno-Ortiz, K. Tsilingiri, P. J. Fernández, M. Mellado, M. T. Díaz-Meco, J. Moscat, M. Serrano, et al. 2009. Regulation of macrophage activation and septic shock susceptibility via p21(WAF1/CIP1). *Eur. J. Immunol*. 39: 810-819.
40. Szwench, E., M. P. Czkowska, K. Marczewski, A. Klisiewicz, I. Micha Owska, I. Ciuba, M. Januszewicz, A. Prejbisz, P. Hoffman, and A. Januszewicz. 2011. Phaeochromocytoma in a 86-year-old patient presenting with reversible myocardial dysfunction. *Blood Press* 20: 383-386.
41. De Vlas, S. J., D. Engels, A. L. Rabello, B. F. Oostburg, L. Van Lieshout, A. M. Polderman, G. J. Van Oortmarssen, J. D. Habbema, and B. Gryseels. 1997. Validation of a chart to estimate true *Schistosoma mansoni* prevalences from simple egg counts. *Parasitology* 114: 113–121.
42. Gaipl, U. S., L. E. Munoz, G. Grossmayer, K. Lauber, S. Franz, K. Sarter, R. E. Voll, T. Winkler, A. Kuhn, J. Kalden, et al. 2007. Clearance deficiency and systemic lupus erythematosus (SLE). *J. Autoimmun.* 28: 114–121.
43. Cvetanovic, M., J. E. Mitchell, V. Patel, B. S. Avner, Y. Su, P. T. van der Saag, P. L. Witte, S. Fiore, J. S. Levine, and D. S. Ucker. 2006. Specific recognition of apoptotic cells reveals a ubiquitous and unconventional innate immunity. *J. Biol. Chem.* 281: 20055–20067.